INTERNATIONAL JOURNAL FOR NUMERICAL METHODS IN FLUIDS, VOL. 17, 145–162 (1993)

AN IMPROVED APPROXIMATION TECHNIQUE TO OBTAIN NUMERICAL SOLUTION OF A CLASS OF TWO-POINT BOUNDARY VALUE SIMILARITY PROBLEMS IN FLUID MECHANICS

N. G. KAFOUSSIAS

Department of Mathematics, University of Patras, 261 10, Patras, Greece

AND

E. W. WILLIAMS

Department of Applied Mathematics and Theoretical Physics, The University, Liverpool L69 3BX, U.K.

SUMMARY

A simple and efficient approximate numerical technique is presented to obtain solutions to a wide class of two-point boundary value similarity problems in fluid mechanics. This technique is based on the common finite difference method with central differencing, a tridiagonal matrix manipulation and an iterative procedure. The technique described in this paper has been successfully applied to three different representative similarity problems of fluid mechanics. Each one of these problems is described by a coupled, non-linear system of three ordinary differential equations and has already been solved elsewhere using a different numerical method. So, the obtained numerical results, by our efficient numerical technique, permit a comparative study and show the accuracy and the effectiveness of this technique.

KEY WORDS Similarity problems Numerical solution methods Finite difference method Iterative procedure

1. INTRODUCTION

Many contemporary problems of interest in fluid mechanics, are reduced, by introduction of suitable similarity or pseudo-similarity variables, to a non-linear and coupled system of ordinary differential equations with their appropriate boundary conditions. A variety of numerical methods have been devised for dealing with such two-point boundary value problems. So, Wang and Kleinstreuer[1] presented a boundary layer analysis of orthogonal free–forced convection on a heated and cooled plate with fluid injection or suction. They used a two-point finite difference technique with Newton's linearization method[2] to solve the dimensionless system of equations and associated boundary conditions. A uniform grid in the ζ-direction was employed with a total of 101 grid points and a variable mesh density was needed in order to accomodate steep gradients near the plate surface. Actually, they solved the finite difference equations of their problem, by the so-called 'Block-elimination method' which is a general one and can be used for any number of first-order equations and for a wide range of boundary conditions. However, the amount of algebra involved in applying this method gets extremely tedious. The laminar mixed convection in a radially rotating semiporous channel was studied by Soong and Hwang.[3] The set of the governing equations was a sixth-order quasilinear system with three boundary conditions at each

0271–2091/93/140145–18$14.00

Received May 1992
Revised March 1993

end of the finite interval $0 \leq y \leq 1$. They converted the boundary-value problem to an initial-value counterpart and solved it by using a fourth-order Runge–Kutta scheme with the modified Newton's method.[4] Shang and Wang[5] studied the effect of variable thermophysical properties on laminar free convection of gas. The governing equations for this type of flow were changed to dimensionless ordinary differential equations by similarity transformations and were solved by a shooting method.[6] Wang[7], using the fifth-order Runge–Kutta–Fehlberg algorithm, obtained a numerical solution of the mixed convection flow problem on a vertical needle with heated tip. He integrated numerically a set of non-linear, ordinary differential equations describing the boundary layers on rotating cones, discs and axisymmetric surfaces with a concentrated heat source using the same algorithm.[8]

Finally, Hassanien and Gorla[9] studied combined forced and free convection in stagnation flows of micropolar fluids over a vertical non-isothermal surfaces. The authors transformed the system of continuity, momentum, angular momentum and energy equations into a coupled non-linear system of three ordinary differential equations, applying the local similarity method and solved it by using Merson's method.

The Runge–Kutta integration scheme, along with the Newton–Raphson shooting method is, therefore, one of the most commonly used algorithms for the solution of such two-point boundary value problems. Even though this method provides satisfactory results for such types of problems, but it may fail when applied to problems in which the differential equations are very sensitive to the choice of the missing initial conditions. On the other hand, a serious difficulty which may be encountered in boundary-value problems is the inherent instability. In Merson's method, integration from one or both ends of the range usually produces rapidly increasing solutions which may occasionally lead to overflow before the matching point is reached.

Another difficulty which often arises is the case in which one end of the range of integration is at infinity. The end-point of integration is usually approximated by assigning a finite value to this point; it is obtained by estimating a value at which the solution will reach its asymptotic state. The computing time for integrating the differential equations can sometimes depend critically on the quality of the initial guesses of the unknown boundary conditions, the locations of the matching point and the infinite end-point.

On the contrary to the above-mentioned numerical methods, the numerical technique we present here has better stability characteristics, is simple, accurate and efficient. The essential features of this technique are the following: (i) It is based on the common finite difference method with central differencing; (ii) on a tridiagonal matrix manipulation; and (iii) on an iterative procedure.

We applied our numerical technique to three particular representative problems which have already been solved by different numerical methods. These problems are the following: (i) Boundary layers on rotating cones, discs and axisymmetric surfaces with a concentrated heat source.[8] (ii) Boundary-layer analysis of orthogonal free–forced convection on a heated and cooled plate with fluid injection or suction.[1] (iii) Combined forced and free convection in stagnation flows of micropolar fluids over vertical non-isothermal surfaces.[9] To test the accuracy and the effectiveness of our numerical technique, we compared our results with those of Wang[8] [problem (i)], Wang and Kleinstreuer[1] [problem (ii)] and Hassanien and Gorla[9] [problem (iii)] and they were found to be in excellent agreement.

2. THE MATHEMATICAL MODELS

In order to demonstrate our numerical technique, three different representative problems of fluid mechanics are solved here. As we stated earlier, each one of these problems has already been

solved by a different numerical method. So, we can compare our results with those obtained by other authors and verify the validity of our numerical technique.

2.1. *First problem*

The first problem we consider is that of the boundary layer on rotating cones, discs and axisymmetric surfaces with a concentrated heat source.[8] The boundary layer equations on a body of revolution are

$$\frac{\partial}{\partial x}(ru)+\frac{\partial}{\partial y}(rv)=0 \qquad \text{(continuity)}, \tag{1}$$

$$\left.\begin{aligned} u\frac{\partial u}{\partial x}+v\frac{\partial u}{\partial y}&=-\frac{1}{\rho}\frac{\mathrm{d}p}{\mathrm{d}x}+\nu\frac{\partial^2 u}{\partial y^2} \qquad (2)\\ u\frac{\partial w}{\partial x}+v\frac{\partial w}{\partial y}+\frac{uw}{r}\frac{\mathrm{d}r}{\mathrm{d}x}&=\nu\frac{\partial^2 w}{\partial y^2} \qquad (3)\end{aligned}\right\} \text{(momentum)},$$

$$u\frac{\partial T}{\partial x}+v\frac{\partial T}{\partial y}=\frac{\nu}{Pr}\frac{\partial^2 T}{\partial y^2} \quad \text{(energy)}, \tag{4}$$

where x, y are intrinsic co-ordinates along and normal to the surface, u, v are the corresponding velocity components, T the temperature, ν the kinematic viscosity, Pr the Prandtl number, w the azimuthal velocity and $r(x)$ the surface distance to the axis of revolution. The surface of revolution is described by the equation

$$r(x)=Ax^s, \tag{5}$$

where A and s are positive constants.

The family of cones are obtained by setting $s=1$ and $A=\sin a$ in equation (5), where $2a$ is the vertex angle. The case $2a=2\pi$ corresponds to the surface of an infinite flat disc. Finally, the heat source, of strength Q, is at the tip $r=x=0$ of the surface of revolution.

Defining now the following transformations:

$$\begin{aligned} &u=A\Omega x^s F'(\eta), \qquad v=-(A\Omega\nu)^{1/2}x^{(s-1)/2}\left\{\frac{3s+1}{2}F+\frac{s-1}{2}\eta F'\right\},\\ &w=A\Omega x^s G(\eta), \quad \theta(\eta)=\frac{T-T_\infty}{Q}x^{(3s+1)/2}\{2\pi\rho c_p A(A\Omega\nu)^{1/2}\}, \qquad (6)\\ &\eta=(A\Omega/\nu)^{1/2}yx^{(s-1)/2} \quad \text{(similarity variable)}, \end{aligned}$$

where ρ is the fluid density, c_p the specific heat, Ω the angular velocity; F, G and θ are the dimensionless stream function, azimuthal velocity and temperature, respectively. Introducing these transformations into equations (1)–(4), we get

$$F'''+s^*FF''+s\{G^2-(F')^2\}=0, \tag{7}$$

$$G''+s^*FG'-2sF'G=0, \tag{8}$$

$$\theta''+s^*Pr(\theta F)'=0, \tag{9}$$

where $s^* = (3s+1)/2$, T_∞ is the fluid temperature away from the surface and primes denote differentiation with respect to $\eta[(\ )' = \mathrm{d}(\ )/\mathrm{d}\eta]$. The boundary conditions for the problem are

$$\begin{aligned} F(0) = F'(0) = \theta'(0) = 0,\ G(0) = 1, \\ F'(\infty) = G(\infty) = \theta(\infty) = 0. \end{aligned} \tag{10}$$

The total heat flux through any surface $x = \text{constant}$, within the boundary layer, is

$$Q = \rho c_p \int_0^\infty 2\pi r u (T - T_\infty)\, \mathrm{d}r, \tag{11}$$

which yields the condition

$$\int_0^\infty F'(\eta)\,\theta(\eta)\,\mathrm{d}\eta = 1. \tag{12}$$

Hence, the system of equations and boundary conditions which describe the problem under consideration, and which hereafter we shall call 'Problem I', is the system of equations (7)–(9), (10) and (12), respectively.

2.2. *Second problem*

As a second mathematical model (hereafter referred as 'Problem II') for applying our numerical technique, we consider the boundary layer analysis of orthogonal free–forced convection on a heated and cooled plate with fluid injection or suction, studied by Wang and Kleinstreuer.[1] The boundary layer equations for a horizontal heated/cooled flat plate aligned parallel to a free stream of velocity u_∞, temperature T_∞ and pressure p_∞, can be written as:

$$\frac{\partial u}{\partial x} + \frac{\partial v}{\partial y} = 0 \qquad \text{(continuity)}, \tag{13}$$

$$\left.\begin{aligned} u\frac{\partial u}{\partial x} + v\frac{\partial u}{\partial y} &= -\frac{1}{\rho}\frac{\mathrm{d}p}{\mathrm{d}x} + \nu\frac{\partial^2 u}{\partial y^2} \\ 0 &= -\frac{1}{\rho}\frac{\partial p}{\partial y} + zg\beta(T - T_\infty) \end{aligned}\right\} \quad \text{(momentum)}, \tag{14, 15}$$

$$u\frac{\partial T}{\partial x} + v\frac{\partial T}{\partial y} = \alpha\frac{\partial^2 T}{\partial y^2} \qquad \text{(energy)}, \tag{16}$$

where g is the acceleration due to gravity, β the coefficient of thermal expansion, z a parameter taking the values $z = 1$ (heated plate) and $z = -1$ (cooled plate) and $\alpha (= k/\rho c_p)$ is the thermal diffusivity.

The associated boundary conditions are

$$\left.\begin{aligned} y = 0\text{:}\quad & u = 0,\quad v = \pm v_w,\qquad T = T_w = \text{constant, or } q_w = -k\left.\frac{\partial T}{\partial y}\right|_{y=0} = \text{constant}, \\ y \to \infty\text{:}\quad & u = u_\infty,\qquad p = p_\infty,\qquad T = T_\infty = \text{constant}, \end{aligned}\right\} \tag{17}$$

where $\pm v_w$ is the injection/suction velocity at the plate. The case $T = Tw =$ constant corresponds to the uniform surface temperature (UST) case, while the case $q_w =$ constant corresponds to the uniform heat flux (UHF) case.

In the present analysis, new mixed convection parameters are introduced for the above-mentioned cases. They index the entire range from pure forced convection ($\zeta = 0$) to pure free convection ($\zeta = 1$) and serve as the dimensionless streamwise co-ordinate. So,

$$\zeta = \begin{cases} (\sigma Ra)^{1/5}/\{\omega Re^{1/2} + (\sigma Ra)^{1/5}\} & \text{for UST case,} \\ (\sigma Ra^*)^{1/6}/\{(\omega Re)^{1/2} + (\sigma Ra^*)^{1/6}\} & \text{for UHF case,} \end{cases} \tag{18}$$

where

$$\sigma = Pr/(1+Pr), \qquad \omega = Pr/(1+Pr)^{1/3}, \qquad Re = u_\infty x/\nu,$$
$$Ra = g\beta|T_w - T_\infty|x^3/(\alpha\nu) \qquad Ra^* = g\beta|q_w|x^4/(\alpha\nu k). \tag{19}$$

Furthermore, the following transformed variables are used to facilitate the numerical solution

$$\eta = y\lambda/x, \qquad \psi = \alpha\lambda F - \int_0^x v_w(x)\,dx, \; G = \sigma(p - p_\infty)x^2/(\rho\alpha\nu\lambda^4), \tag{20}$$

$$\theta = (T - T_\infty)/(T_w - T_\infty) \quad \text{for UST case,} \tag{21}$$

and

$$\theta = (T - T_\infty)/\{q_w x/(k\lambda)\} \quad \text{for UHF case.} \tag{22}$$

The dimensionless buoyancy parameter λ, is defined as

$$\lambda = \begin{cases} (\omega Re)^{1/2} + (\sigma Ra)^{1/5} = (\omega Re)^{1/2}/(1-\zeta_T) = (\sigma Ra)^{1/5}/\zeta_T & \text{for UST case,} \\ (\omega Re)^{1/2} + (\sigma Ra^*)^{1/6} = (\omega Re)^{1/2}/(1-\zeta_q) = (\sigma Ra^*)^{1/6}/\zeta_q & \text{for UHF case.} \end{cases} \tag{23}$$

The dimensionless mass transfer or blowing/suction parameter MP, is defined as

$$\mathrm{MP} = \pm\frac{x v_w}{\alpha\lambda}. \tag{24}$$

In assuming MP to be constant, the wall velocity varies along the plate. Specifically

$$v_w \sim \begin{cases} c_1 x^{-1/2} + c_2 x^{-2/5} & \text{for UST case,} \\ c_3 x^{-1/2} + c_4 x^{-2/3} & \text{for UHF case,} \end{cases} \tag{25}$$

where c_i, $i = 1, 2, 3, 4$, are constants.

Using the stream function approach, $u = \partial\Psi/\partial y$, $v = -\partial\Psi/\partial x$, the continuity equation is automatically satisfied. Substituting equations (20)–(22) into equations (14)–(17) we obtain

$$PrF''' + aFF'' - bF'^2 + (1+Pr)\{c\eta G' - dG\} - \mathrm{MP}F'' = e\left\{F'\frac{\partial F'}{\partial\zeta} - F''\frac{\partial F}{\partial\zeta} + (1+Pr)\frac{\partial G}{\partial\zeta}\right\}, \tag{26}$$

$$G' = zf\theta \tag{27}$$

and

$$\theta'' + aF\theta' - nF'\theta - \mathrm{MP}\theta' = e\left\{F'\frac{\partial\theta}{\partial\zeta} - \theta'\frac{\partial F}{\partial\zeta}\right\}, \tag{28}$$

$$F(\zeta,\theta) = F'(\zeta,0) = 0 \quad \text{and} \quad \theta(\zeta,0) = 1 \quad \text{or} \quad \theta'(\zeta,0) = -1,$$
$$F'(\zeta,\infty) = (1+Pr)^{1/3}(1-\zeta)^2, \qquad G(\zeta,\infty) = 0 \quad \text{and} \quad \theta(\zeta,\infty) = 0. \tag{29}$$

In the above equations, primes denote differentiation with respect to the similarity variable η. Also, the coefficients in equations (26)–(29) are defined as follows:

$$\begin{aligned} &a=(5+\zeta)/10, \quad b=\zeta/5, \quad c=(5-\zeta)/10, \quad d=2\zeta/5, \\ &e=\zeta(1-\zeta)/10, \quad f=\zeta^5, \quad n=0, \quad \zeta=\zeta_T \text{ for UST case} \end{aligned} \tag{30}$$

and

$$\begin{aligned} &a=(3+\zeta)/6, \quad b=\zeta/3, \quad c=(3-\zeta)/6, \quad d=2\zeta/3, \\ &e=\zeta(1-\zeta)/6, \quad f=\zeta^6, \quad n=(3-\zeta)/6, \quad \zeta=\zeta_q \text{ for UHF case} \end{aligned} \tag{31}$$

For the special case of pure free convection ($\zeta=1$) and for the UST-case, the non-similar equations (26)–(28) are reduced to the following similarity equations:

$$PrF'''+\tfrac{3}{5}FF''-\tfrac{1}{5}F'^2-\tfrac{2}{5}(1+Pr)(\eta G'-G)-\mathrm{MP}F''=0, \tag{32}$$

$$\theta''+\tfrac{3}{5}F\theta'-\mathrm{MP}\theta=0 \tag{33}$$

and

$$G'=z\theta. \tag{34}$$

In this case the corresponding boundary conditions become

$$\begin{aligned} &F(0)=F'(0)=0, \quad \theta(0)=1, \\ &F'(\infty)=0, \quad G(\infty)=0, \quad \theta(\infty)=0. \end{aligned} \tag{35}$$

The system of equations (32)–(35) will be used for our numerical technique (Problem II).

2.3 Third problem

As a third and last application of our numerical technique, the problem of combined forced and free convection in stagnation flows of micropolar fluids over vertical non-isothermal surfaces is solved (hereafter referred as 'Problem III'). This problem is governed by the following set of partial differential equations

$$u_{,x}+v_{,y}=0 \quad \text{(continuity)}, \tag{36}$$

$$uu_{,x}+vu_{,y}=-\frac{1}{\rho}\frac{\mathrm{d}p}{\mathrm{d}x}+\nu u_{,yy}+\frac{\kappa}{\rho}N_{,y}\pm g\beta(T-T_\infty) \text{ (momentum)}, \tag{37}$$

$$uN_{,x}+vN_{,y}=-\frac{\kappa}{\rho j}(2N+u_{,y})+\frac{\gamma}{\rho j}N_{,yy} \quad \text{(angular momentum)}, \tag{38}$$

$$uT_{,x}+vT_{,y}=\alpha T_{,yy} \quad \text{(energy)}, \tag{39}$$

where N is the angular velocity, κ, γ are material constants, j is the microinertia per unit mass and

$$(\ )_{,x}=\frac{\partial(\ )}{\partial x}, \quad (\ )_{,y}=\frac{\partial(\ )}{\partial y} \quad \text{and} \quad (\ )_{,yy}=\frac{\partial^2(\ )}{\partial y^2}.$$

The boundary conditions for the velocity and temperature field are given by the following:

$$\begin{aligned} &y=0: \quad u=0, \quad v=0, \quad N=0, \quad T=T_w(x), \\ &y\to\infty: \quad u=U_\infty, \quad N=0, \quad T=T_\infty, \end{aligned} \tag{40}$$

Finally, the plus sign, in the last term of the momentum equation, indicates buoyancy assisting the flow, whereas the negative sign stands for buoyancy opposing the flow.

Introducing a stream function ψ such that

$$u=\psi_{,y} \quad \text{and} \quad v=-\psi_{,x} \tag{41}$$

the continuity equation (36) is automatically satisfied. We now introduce the following dimensionless quantities:

$$\eta=y(a/\nu)^{1/2}, \qquad \xi=\frac{\rho\beta(T_w-T_\infty)}{a^2x}=\frac{Gr_x}{Re_x^2}, \qquad F(\xi,\eta)=x^{-1}\psi(\nu a)^{-1/2},$$

$$G(\xi,\eta)=x^{-1}\left(\frac{a^3}{\nu}\right)^{-1/2}N, \qquad \theta=\frac{T-T_\infty}{T_w-T_\infty}, \qquad \Delta=\kappa/\mu, \qquad \lambda=\gamma/\mu j, \tag{42}$$

$$B=\gamma/\alpha j, \qquad Gr_x=g\beta(T_w-T_\infty)x^3/\nu^2 \quad \text{a local Grashof number,}$$

where $Re_x=U_\infty x/\nu$ is a local Reynolds number, $a=$proportionality constant and B, Δ, λ are dimensionless material parameters. Assuming that along the stagnation line the terms containing $(\ )_{,\xi}$ are negligible (local similarity approach to the stagnation point problem), the system of equations (37)–(39) becomes

$$(1+\Delta)F'''+FF''-(F')^2+\Delta G'=-1\mp\xi\theta, \tag{43}$$

$$\lambda G''-\Delta B(2G+F'')-GF'+FG'=0, \tag{44}$$

$$\theta''+Pr\,F\theta'=Pr\left\{x\frac{dT_w}{dx}F'\theta\right\}\Big/(T_w-T_\infty), \tag{45}$$

where Pr is the Prandtl number and primes indicate differentiation with respect to η. It is noted that a similarity solution exists if $[T_w(x)-T_\infty]=bx^n$, $n=0$ or $n=1$. The case $n=1$ corresponds to an exact similarity solution, while the case $n=0$ to a local similarity one. So, the problem under consideration along with restrictions given by

$$T_w(x)-T_\infty=bx^n, \quad n=0, 1 \tag{46}$$

may be written as

$$(1+\Delta)F'''+FF''-(F')^2+\Delta G'+1\pm\xi\theta=0, \tag{47}$$

$$\lambda G''-\Delta B(2G+F'')-GF'+FG'=0, \tag{48}$$

$$\theta''+Pr\,F\theta'-n\,Pr\,F'\theta=0, \tag{49}$$

$$F(\xi,0)=F'(\xi,0)=0, \qquad G(\xi,0)=0, \qquad \theta(\xi,0)=1,$$

$$F'(\xi,\infty)=1, \qquad G(\xi,\infty)=0, \qquad \theta(\xi,\infty)=0. \tag{50}$$

3. NUMERICAL SOLUTION METHOD

The purpose of this work is the development of a new approximate technique, to calculate the numerical solution of a class of similarity problems in fluid mechanics. We first demonstrate this technique by solving the system of equations (7)–(9) of Problem I.

3.1. Problem I

Equation (7) can be written as

$$F''' + s^* FF'' - sF'F' = -sG^2. \tag{51}$$

So, it can be considered as a second-order linear ordinary differential equation in $y = F'(\eta)$ if $G(\eta)$ and an approximation $F(\eta)$ [or $F'(\eta)$] are known. In this case equation (51) can be written as

$$(F')'' + s^* F(F')' - sF'(F') = -sG^2 \quad \text{or} \quad y'' = p(\eta)y' + q(\eta)y + r(\eta), \tag{52}$$

where $y(\eta) = F'(\eta)$, $p(\eta) = -s^* F(\eta)$, $q(\eta) = sF'(\eta)$ and $r(\eta) = -sG^2(\eta)$. Equation (52) can be solved now by a common finite difference method, based on central differencing and tridiagonal matrix manipulation. It can be shown[10] that when using the above-mentioned difference method, in the case where p, q and r are continuous functions of η on the closed interval $[0, \eta_\infty]$, with $q(\eta) \geq 0$ on this interval, then the solution to equation (52), together with boundary conditions $y(0) = a$ and $y(\eta_\infty) = \beta$, where a, β are real constants, is unique provided the step size $h < 2/L$, where $L = \max|p(\eta)|$, $0 \leq \eta \leq \eta_\infty$. On the other hand it is necessary to establish that $y^{(4)}$ is continuous on $[0, \eta_\infty]$ in order to ensure that the truncation error of this method has order $O(h^2)$.

Hence, to start the solution procedure it is necessary to assume distribution curves for $F'(\eta)$ and $G(\eta)$ between $\eta = 0$ and $\eta = \eta_\infty$ ($\eta \to \infty$) which satisfy the boundary conditions (10). These selected curves can be quite arbitrary as long as they satisfy the boundary conditions. For example, $F'(\eta) = (1 - \eta/\eta_\infty)(\eta/\eta_\infty)$ and $G(\eta) = (1 - \eta/\eta_\infty)$ can be used as first inputs. The $F(\eta)$ distribution is obtained by integrating the assumed $F'(\eta)$ curve. $G(\eta)$ is then retained, whilst the momentum equation (51) is solved, using an algorithm employing a tridiagonal scheme, enabling a new approximation for $F'(\eta)$ to be produced. The $F(\eta)$ distribution is updated by integrating the new $F'(\eta)$ curve. These new profiles of $F'(\eta)$ and $F(\eta)$ are then used for new inputs and so on. So, the momentum equation (52) is solved iteratively until convergence is attained. The criterion of convergence involves the values of the physically important gradient $F''(0)$. The iterations stop when the difference in the values of $F''(0)$, between two successive iterations, are less than a small quantity ε.

The converged profile of $F'(\eta)$ [or $F(\eta)$] is then used to solve equation (8), using the same algorithm, but without iterations now, producing thus a new approximation for $G(\eta)$. In this case we have $y(\eta) = G(\eta)$.

Next, the computational procedure reverts to its original starting point using the most current distributions of $F'(\eta)$ and $G(\eta)$ as inputs. This process is continued until final convergence is attained viz. the changes in $F''(0)$ and $G'(0)$ are within a certain specified tolerance ε of, say, less than 10^{-5} in magnitude. After $F(\eta)$ is obtained the solution of the energy equation (9) under boundary conditions (10) and (12) can easily be obtained. Equation (9) can be written as

$$\theta'' + s^* Pr F\theta' + s^* Pr F'\theta = 0 \tag{53}$$

So, equation (53) is a second-order linear ordinary differential equation in $y(\eta) = \theta(\eta)$, with known coefficients. Consequently, it can be solved at once by applying the above-mentioned algorithm. In order to apply our numerical technique a proper step size $h = \Delta\eta$ and an appropriate η_∞ value, as an approximation to $y = \infty$, are determined by the trial-and-error method, the criterion being the stability of physically important gradients $F''(0)$ and $G'(0)$. It was found that a step size $\Delta\eta = 0{\cdot}025$ is sufficient to provide accurate numerical results. Sometimes, to avoid divergence of the iterative procedure, as applied to the momentum equation, under-relaxation is employed, with an under-relaxation factor of 0·5. The whole numerical procedure is shown in a flow-chart presented in Figure 1 for a more general case of a boundary value problem (Problem III).

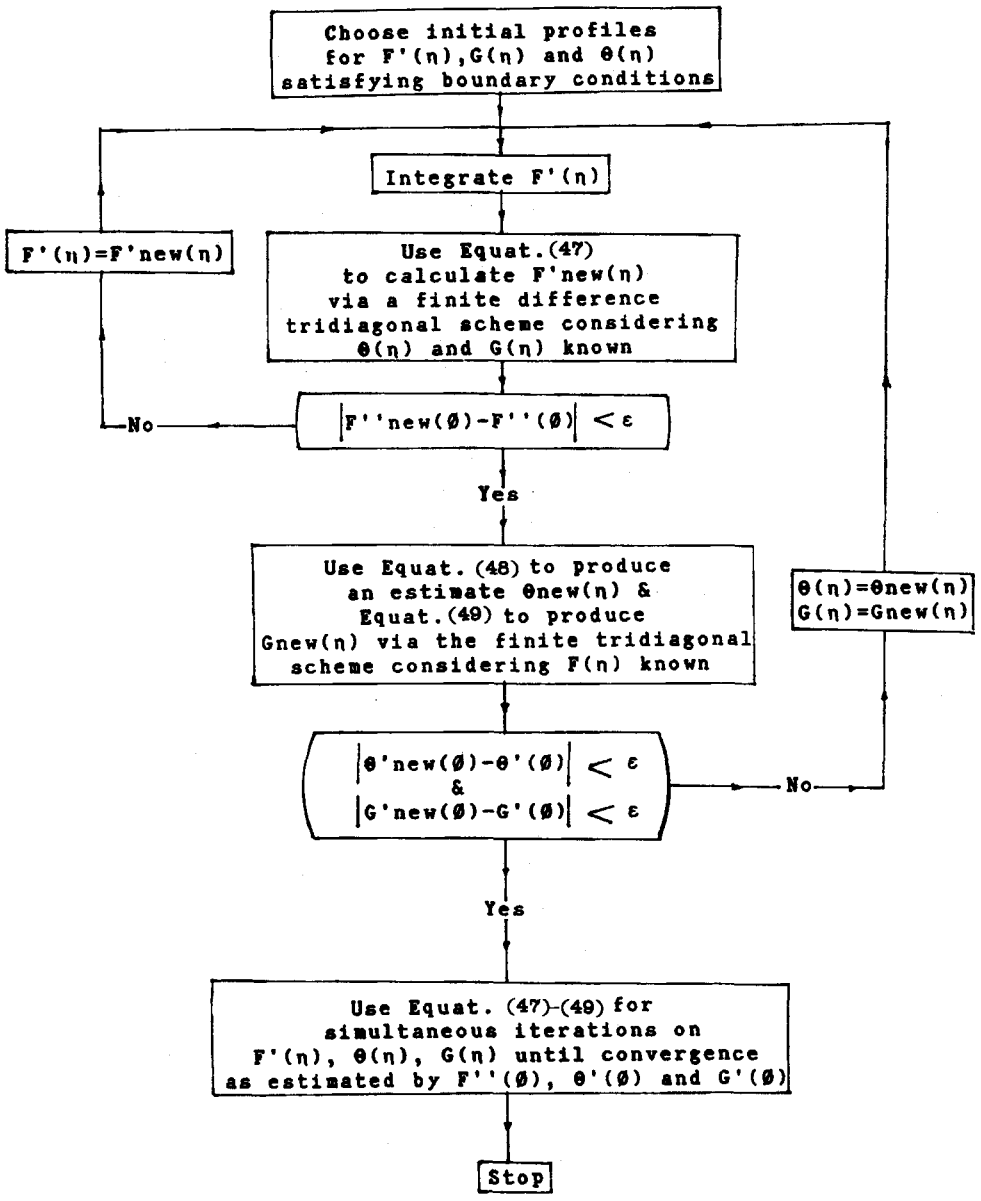

Figure 1. Flow chart of the computer program for the approximation numerical technique

3.2. Problem II

We can proceed now to apply our numerical technique, in a similar manner, to solve the system of equations (32)–(34) subject to boundary conditions (35). The momentum equation (32) can be written as

$$y'' = p(\eta)y' + q(\eta)y + r(\eta), \tag{54}$$

where

$$y=F'(\eta),\quad p(\eta)=(\mathrm{MP}-3F/5)/Pr,\qquad q(\eta)=F'/5Pr$$

and

$$r(\eta)=-2(1+Pr)(\eta G'-G)/5Pr.$$

Hence, equation (32) can be solved by exactly the same method as equation (52). To start the numerical procedure we assume distribution curves $F'(\eta)$ and $\theta(\eta)$ satisfying their boundary conditions (35). The F distribution is obtained by integrating the assumed $F'(\eta)$ curve, whereas the G' distribution is already known from equation (34). The function $G(\eta)$ is then obtained by integrating the $G'[=\theta(\eta)]$ distribution, using the condition $G(\infty)=0$. After that, the momentum equation is solved iteratively and the whole procedure is continued in a quite similar manner as in Problem I. The convergence criterion for the solution here also involves values of the physically important gradients $F''(0)$, $\theta'(0)$ and $G'(0)$.

It is worth noting that the momentum equation in Problem I, as well as in Problem II, contains only the unknown function G (and/or G'). In Problem I, G is the non-dimensional azimuthal velocity; whereas in Problem II, G' is the non-dimensional temperature. So, the iterative procedure takes place, mainly, between the two first equations of the systems (7)–(9) and (32)–(34) governing Problems I and II, respectively.

3.3 Problem III

A more general case is presented in the solution of this problem. It is known that in free convection problems there is a flow-thermal coupling. In this case the momentum equation (47), contains not only the dimensionless microrotation G, but the dimensionless temperature θ as well. So, the system of equations (47)–(49) is more general than the previous ones and the solution methodology of this problem, constitutes a generalization of our numerical technique.

In the system of equations (47)–(49) we have also to consider the variation of the following parameters: (i) the Prandtl number Pr, (ii) the buoyancy parameter ξ, (iii) the integer n and (iv) the dimensionless material parameters B, λ and Δ. During the course of the numerical solution of the system (47)–(50) all these dimensionless parameters take various values. The values of the integer $n=0$ and $n=1$ correspond to the isothermal wall case and the linear wall temperature case, respectively.

We proceed now to solve the system of equations (47)–(49) as follows. Equation (47) can be considered as a second-order linear ordinary differential equation in $F'(\eta)$ if $G(\eta)$, $\theta(\eta)$ and an approximation to $F(\eta)$ and $F'(\eta)$ are known. For instance, equation (47) can be written as

$$(1+\Delta)(F')''+F(F')'-F'(F')=-\Delta G'-1\mp\xi\theta \tag{55}$$

or

$$y''(\eta)=p(\eta)\,y'(\eta)+q(\eta)\,y(\eta)+r(\eta), \tag{56}$$

where

$$y(\eta)=F'(\eta),\ p(\eta)=-F(\eta)/(1+\Delta),\ q(\eta)=F'(\eta)\,|\,(1+\Delta)\ \text{and}\ r(\eta)=(-\Delta G'-1\mp\xi\theta)\,|\,(1+\Delta). \tag{57}$$

So, it can be solved by the above-mentioned finite difference method based on central differencing and tridiagonal matrix manipulation. To start the solution procedure, for given values of the dimensionless parameters Pr, B, Δ, λ and ξ, it is again necessary to assume distribution curves for F', G and θ between $\eta=\theta$ and $\eta=\eta_\infty$. The selected curves can be quite arbitrary as long as they

satisfy the boundary conditions (50). The F distribution is obtained by integrating the assumed F' curve. In this case G and θ distributions are then held fixed and the momentum equation (47) or (55) is solved iteratively, as in Problem I, enabling a new approximation for $F'(\eta)$ to be produced. The converged profile of $F'(\eta)$ is integrated again and the new profiles of $F'(\eta)$ and $F(\eta)$ are then used to solve the equations (48) and (49), using the same algorithm but without iterations now, producing thus a new approximation for $G(\eta)$ and $\theta(\eta)$. Next, the computational procedure reverts to its starting point using the most current distributions of $F'(\eta)$, $G(\eta)$ and $\theta(\eta)$ as inputs. This process is continued until final convergence of the solution is attained viz. the changes in $F''(0)$, $-G'(0)$ and $-\theta'(0)$ are with the given tolerance ε. The whole numerical procedure is shown in the flow-chart of Figure 1.

In the numerical computations, a proper step size $\Delta\eta$ and an appropriate η_∞ value (an approximation to $\eta=\infty$ in the free stream) must be determined, usually by a trial-and-error approach. It is known that the location of the boundary-layer edge, η_∞, is strongly dependent on the Prandtl number Pr. In general, if the appropriate η_∞ value is not known, it is advantageous to start the computation by using a small value of η_∞ (say, 4 or smaller) and then successively increase the η_∞ value until convergence is obtained, the criterion being the stability of the physically important gradients $F''(0)$, $-G'(0)$ and $-\theta'(0)$. Once a proper η_∞ value is determined, a check of the effect of step size $h=\Delta\eta$ on the numerical values of the above-mentioned gradients should be conducted. Usually, a step size of $\Delta\eta=0{\cdot}025$ was sufficient to provide accurate numerical results in all problems under consideration. It should be noted that although experience has shown that by forward integration in conjuction with a shooting method, too small or too large an η_∞ value, will give rise to difficulties in convergence, but in our case we did not face such a problem. The stability is the main characteristic of our numerical technique.

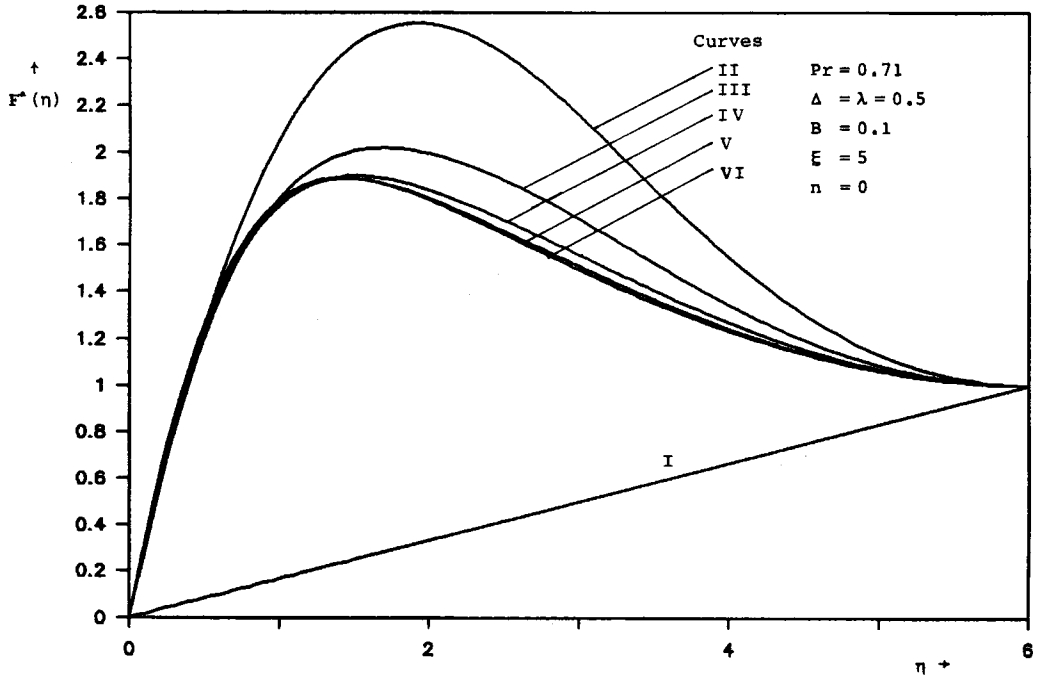

Figure 2. The first six approximative curves for the velocity profile $F'(\eta)$, of Problem III, for linear variation of the guessed temperature $[\theta(\eta)]$ and angular velocity profiles $[G(\eta)]$

On the other hand, although finite difference methods generally require more work to obtain a specified accuracy compared to the classic forward integration schemes in conjuction with a shooting method, the computational efficiency of our method is quite satisfactory. Figure 2 shows the first six approximative curves for the velocity profile $F'(\eta)$ of Problem III, for linear variation of the guessed dimensionless temperature $[\theta(\eta)]$ and angular velocity profiles $[G(\eta)]$. It is evident that convergence to the solution is very fast.

4. REPRESENTATIVE RESULTS AND DISCUSSION

To test the accuracy and the applicability of our method, some numerical calculations were carried out for different values of the dimensionless parameters in the problems under consideration. Our representative results are shown in Figures 3–7 and in Tables I–V.

4.1. Problem I

Table I shows the values of the normalized maximum temperature $\theta(0)$ for $s=1$ and for various values of Prandtl number Pr. Case I corresponds to the results obtained by Wang,[8] using the fifth-order Runge–Kutta–Fehlberg method in conjuction with a two-dimensional shooting method, whereas case II corresponds to the results obtained by the technique presented here. From this table one can see that our results are in a very good agreement with those obtained by Wang,[8] since the maximum relative error is less than 0·27% ($Pr=200$). Table II shows the initial and final values of the flow field and the maximum temperature $\theta(0)$ for various values of parameter s and Prandtl number Pr. The maximum relative error in this case is less than 0·078%

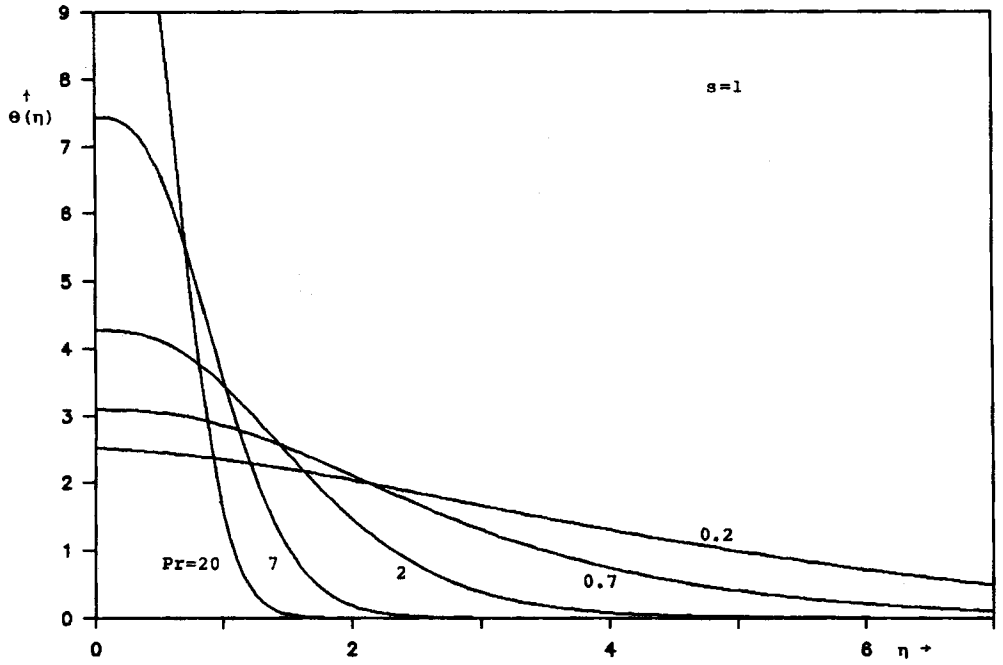

Figure 3. Similarity temperature function $\theta(\eta)$ for various Prandtl numbers Pr ($s=1$)

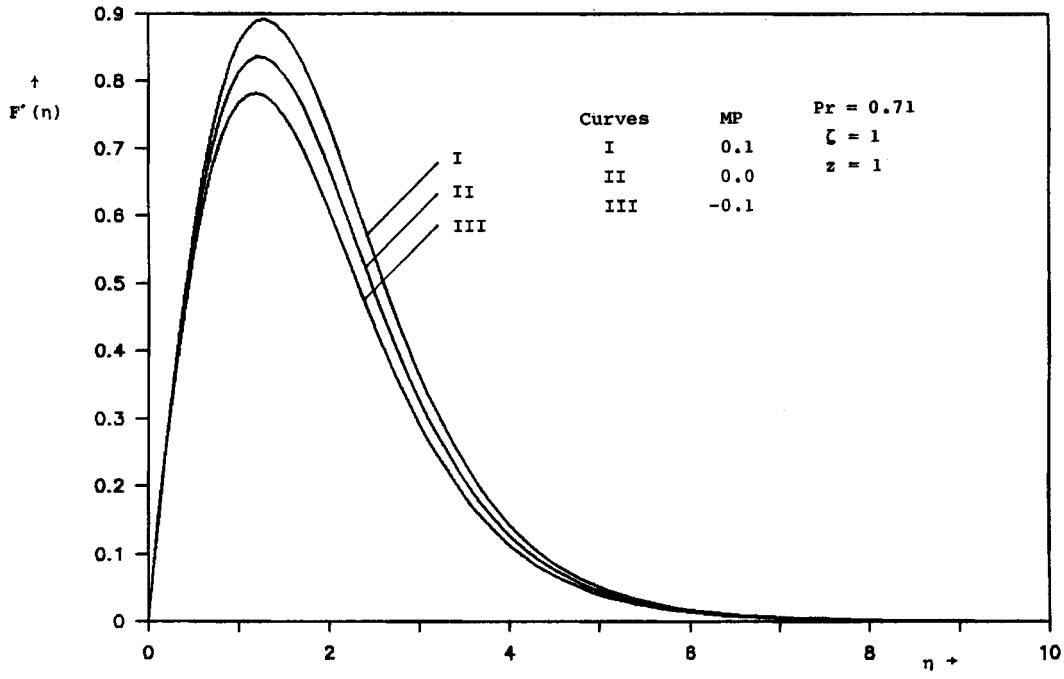

Figure 4. Variation of the dimensionless velocity profiles $F'(\eta)$ for different values of the mass transfer parameter MP.

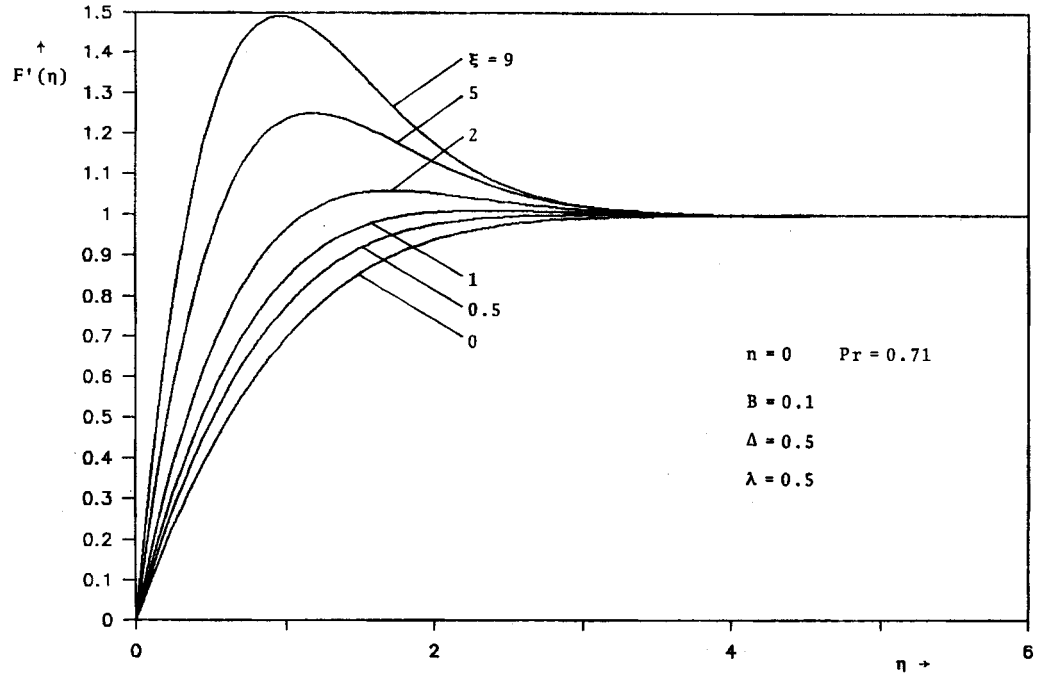

Figure 5. Velocity distribution (buoyancy-assisted case)

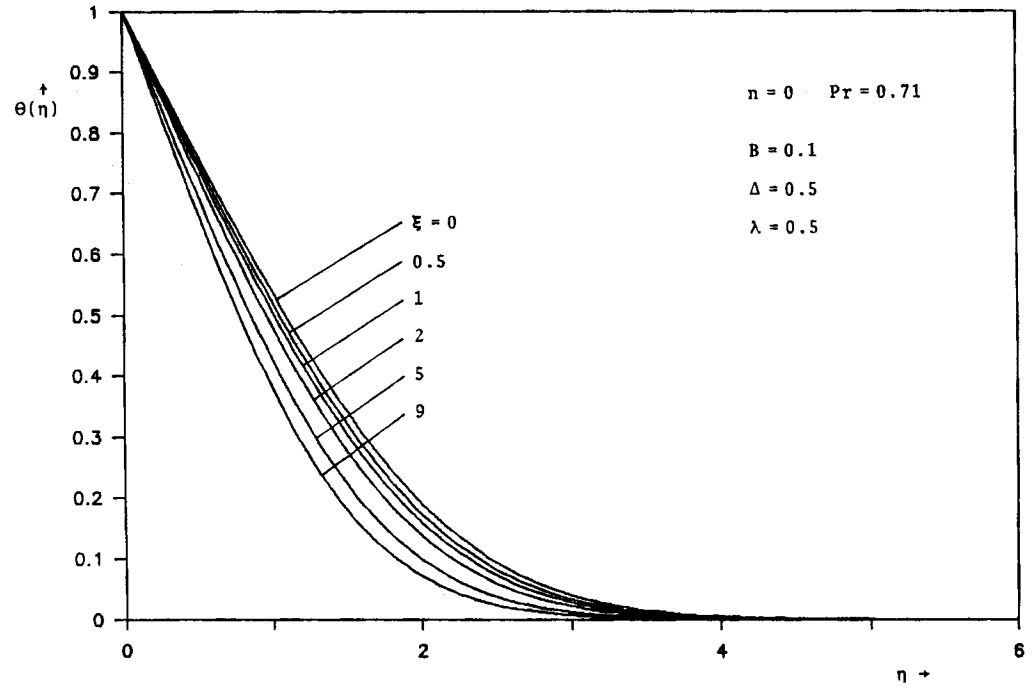

Figure 6. Temperature distribution (buoyancy-assisted case)

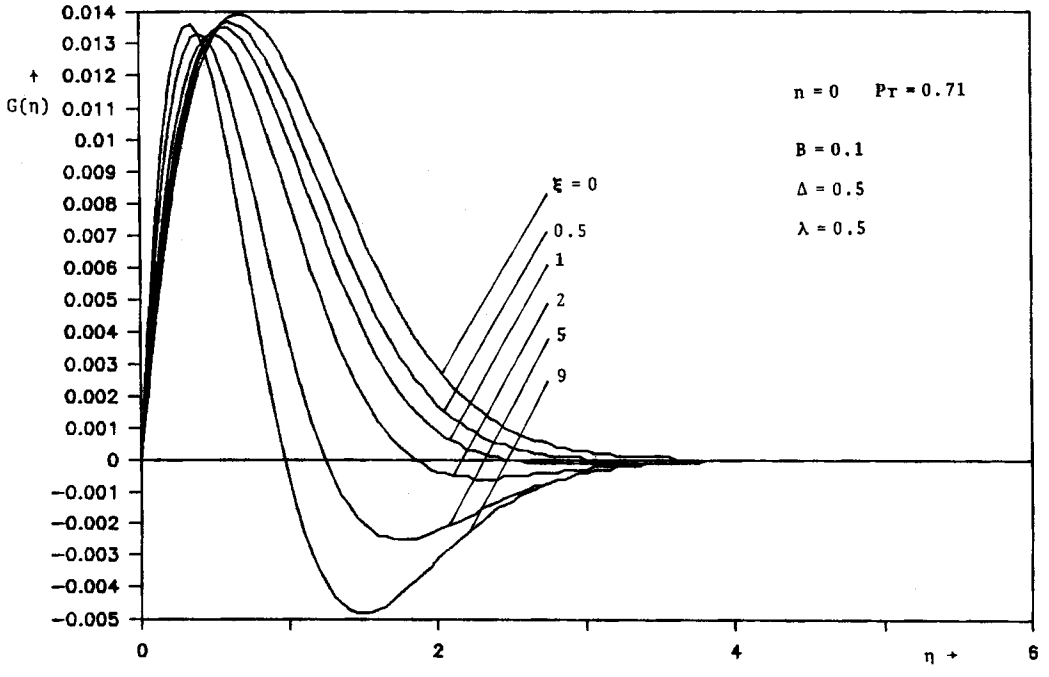

Figure 7. Microrotation distribution (buoyancy-assisted case)

Table I. Values of the normalized maximum temperature $\theta(0)$ for $s=1$ and various Prandtl numbers

Pr	0·07	0·2	0·7	2	7	20	70	200
$\theta(0)$								
Case I	2·3554	2·5224	3·0915	4·2706	7·4326	12·9880	26·9690	51·3830
Case II	2·3599	2·5254	3·0929	4·2714	7·4341	12·9938	27·0004	51·5215

Table II. Initial and final values of the flow field and maximum temperature $\theta(0)$ for various values of s and Pr

		$s=1·25$	$s=1·5$	$s=2$
	Case I	0·5736	0·6307	0·7317
$F''(0)$	Case II	0·5736	0·6306	0·7316
	Case I	−0·6864	−0·7503	−0·8641
$G'(0)$	Case II	−0·6864	−0·7504	−0·8642
	Case I	0·4060	0·3777	0·3366
$F(\infty)$	Case II	0·4068	0·3791	0·3371
Pr			$\theta(0)$	
	Case I	2·7424	2·9447	3·3080
0.2	Case II	2·7397	2·9398	3·3058
	Case I	3·3553	3·6000	4·0455
0.7	Case II	3·3546	3·5987	4·0449
	Case I	4·6291	4·9631	5·5734
2	Case II	4·6293	4·9631	5·5737
	Case I	8·0451	8·6169	9·6642
7	Case II	8·0466	8·6189	9·6672
	Case I	14·044	15·030	16·838
20	Case II	14·0510	15·0404	16·8551

Table III. Wall shear stress and Nusselt number for pure free convection from a horizontal impermeable (MP=0) plate for different Prandtl numbers

	$\bar{F}''(0)$		$-\bar{\theta}'(0)$	
Pr	Case I	Case II	Case I	Case II
0·71	0·8907	0·9033	0·5923	0·5900
1	0·7870	0·7939	0·6472	0·6472
10	0·3320	0·3349	1·1329	1·1329

$$\bar{F}''(0)=(6.25)^{1/5}\, Pr^{-2/5}\, \sigma^{3/5}\, F''(0) \quad \sigma=Pr/(1+Pr)$$
$$\bar{\theta}'(0)=(12.5\,\sigma Pr)^{1/5}\,\theta'(0)$$

Table IV. Local friction factor, wall couple stress and Nusselt number for $n=1$ (linear variation of the wall temperature)

			Buoyancy-opposed flow					
			Case I			Case II		
Pr	λ	Δ	$F''(0)$	$-G'(0)$	$-\theta'(0)$	$F''(0)$	$-G'(0)$	$-\theta'(0)$
0·7	0·5	0·5	0·59849	0·04054	0·60899	0·59849	0·04054	0·60898
		1·5	0·48659	0·10168	0·57764	0·48658	0·10168	0·57765
		4·5	0·33474	0·20183	0·53060	0·33473	0·20182	0·53059
	1·5	0·5	0·59974	0·01743	0·60887	0·59974	0·01743	0·60889
		1·5	0·49160	0·04569	0·57678	0·49158	0·04569	0·57678
		4·5	0·34427	0·09916	0·52659	0·34418	0·09915	0·52659
10.0	0·5	0·5	0·79971	0.04602	1·66850	0·79974	0·04602	1·66886
		1·5	0·62968	0·11547	1·55074	0·62969	0·11547	1·55102
		4·5	0·41589	0·23050	1·37784	0·41587	0·23047	1·37800
	1·5	0·5	0·80098	0·01926	1·66861	0·80101	0·01926	1·66899
		1·5	0·63495	0·05045	1·55080	0·63494	0·05045	1·55106
		4·5	0·42644	0·11003	1·37422	0·42645	0·11003	1·37441

Table V. Local friction factor, wall couple stress and Nusselt number for $n=1$ (linear variation of the wall temperature)

			Buoyancy-assisted flow					
			Case I			Case II		
Pr	λ	Δ	$F''(0)$	$-G'(0)$	$-\theta'(0)$	$F''(0)$	$-G'(0)$	$-\theta'(0)$
0·7	0·5	0·5	1·36189	0·05452	0·72379	1·36189	0·05425	0·72383
		1·5	1·01633	0·13631	0·67393	1·01633	0·13631	0·67395
		4·5	0·62920	0·27581	0·60227	0·62919	0·27579	0·60228
	1·5	0·5	1·36310	0·02186	0·72368	1·36310	0·02186	0·72371
		1·5	1·02165	0·05725	0·67319	1·02164	0·05725	0·67323
		4·5	0·64102	0·12604	0·59863	0·64103	0·12604	0·59865
10.0	0·5	0·5	1·19444	0.05000	1·82076	1·19438	0·05001	1·82120
		1·5	0·89489	0·12545	1·67286	0·89486	0·12546	1·67322
		4·5	0·55822	0·25228	1·46440	0·55819	0·25226	1·46462
	1·5	0·5	1·19563	0·02045	1·82082	1·19557	0·02045	1·82187
		1·5	0·90002	0·05350	1·67281	0·89999	0·05350	1·67316
		4·5	0·56923	0·11716	1·46107	0·56920	0·11716	1·46129

($s=2$, $Pr=20$). It is worth noting that the maximum error between cases I and II is presented for the largest value of the Prandtl number Pr. Finally, Figure 3 shows the variation of dimensionless temperature $\theta(\eta)$ for various values of Prandtl number Pr at $s=1$. It is observed that the temperature field in our case is exactly the same as that of Wang.[8]

4.2. *Problem II*

In this case the problem under consideration is the special case of the pure free convection ($\zeta = 1$) on a heated plate ($z = 1$) with uniform surface temperature (UST case) and with non-linear fluid injection or suction. So, the only dimensionless parameters entering into this problem are the Prandtl number *Pr* and the mass transfer (blowing/suction) parameter MP. The value MP = 0 corresponds to an impermeable plate. The numerical results obtained by our approximation technique (case II), are compared with data published by Wang and Kleinstreuer[1] (case I), for special case studies, and are presented in Table III and Figure 4. So, Table III shows the values of the dimensionless coefficients $\bar{F}''(0)$ and $-\bar{\theta}'(0)$ for the wall shear stress and Nusselt number, respectively, for different values of the Prandtl number *Pr*, for both cases I and II. On the other hand, Figure 4 shows the variation of the dimensionless velocity profiles $F'(\eta)$ on an isothermal horizontal plate for pure free convection for different values of the mass transfer parameter MP. From Table III one can see that the values of the dimensionless coefficient $-\bar{\theta}'(0)$ (Nusselt number), obtained by the numerical technique presented here (case II), are in excellent agreement with those of case I, whereas the maximum relative error in the values of the wall stress coefficient $\bar{F}''(0)$, is less than 1·41%.

4.3. *Problem III*

This is a representative problem for applying our numerical technique and verifying its applicability and effectiveness. Hence, a more detailed analysis is presented in this case and our representative results are shown in Figures 5–7 and in Tables IV and V. Figures 5, 6 and 7 show the variation of the velocity profile $F'(\eta)$, temperature profile $\theta(\eta)$ and microrotation profile $G(\eta)$, respectively, for the isothermal wall ($n = 0$) and the buoyancy assisted case. Tables IV and V show the variations of the local friction factor $F''(0)$, the wall couple stress $-G'(0)$ and Nusselt number $-\theta'(0)$, for buoyancy opposed and buoyancy assisted flow, respectively, and for the case of the linear variation of the wall temperature ($n = 1$). Case I corresponds to the results obtained by Merson's method, while case II corresponds to the results obtained by the method presented here.

The behaviour of the flow field, for the problem under consideration, has been extensively studied by Hassanien and Gorla,[9] and hence further discussion would appear to be redundant. Consequently, we restrict attention to the accuracy of the obtained results. A detailed examination of the values of the physically important gradients $F''(0)$, $-G'(0)$ and $\theta'(0)$ in Table IV or V for Cases I and II, proves that our results are in excellent agreement with those obtained by the above-mentioned authors, since the maximum error is less than 0·03%.

5. CONCLUSIONS

This work has shown that the described numerical technique is capable of solving a wide class of two-point boundary value similarity problems in fluid mechanics. It is based on the common finite difference method with central differencing, a tridiagonal matrix manipulation and an iterative procedure. So, it can be programmed and applied easily. The whole numerical scheme is stable, accurate and rapidly converging. These facts suggest this is a powerful and accurate method suitable for application to a wide class of two-point boundary value similarity problems in fluid mechanics.

REFERENCES

1. T. Y. Wang and C. Kleinstreuer, 'Boundary-layer analysis of orthogonal free–forced convection on a heated and a cooled plate with fluid injection or suction', *Int. J. Eng. Sci.*, **28**, 437–450 (1990).
2. T. Cebeci and P. Bradshow, *Momentum Transfer in Boundary Layer*, Hemisphere, Washington, DC, 1977.

3. C. Y. Soong and G. J. Hwang, 'Laminar mixed convection in a radially rotating semiporous channel', *Int. J. Heat Mass Transfer*, **33**, 1805–1816 (1990).
4. M. Rahman, 'On the numerical solution of the flow between a rotating and a stationary disk', *J. Comput. Appl. Math.*, **4**, 289–293 (1978).
5. D. Y. Shang and B. X. Wang, 'Effect of variable thermophysical properties on laminar free convection of gas', *Int. J. Heat Mass Transfer.*, **33**, 1387–1395 (1990).
6. I. Gladwell and D. K. Sayers, *Computational Techniques for Ordinary Differential Equations*, Academic Press, London, 1980.
7. C. Y. Wang, 'Mixed convection on a vertical needle with heated tip', *Phys. Fluids A*, **2**, 622–625 (1990).
8. C. Y. Wang, 'Boundary layers on rotating cones, discs and axisymmetric surfaces with a concentrated heat source', *Acta Mechanica*, **81**, 245–251 (1990).
9. I. A. Hassanien and R. S. R. Gorla, 'Combined forced and free convection in stagnation flows of micropolar fluids over vertical non-isothermal surfaces', *Int. J. Eng. Sci.*, **28**, 783–792 (1990).
10. R. L. Burden, J. D. Faires and A. C. Reynolds, *Numerical Analysis*, 2nd edn., Prindle, Weber and Schmidt, Boston, Massachusetts, 1981.